11242 *Inorg. Chem.* **2009**, *48*, 11242–11250
DOI: 10.1021/ic901663w

Inorganic Chemistry
Article

Circularly Polarized Luminescence of Eu(III) Complexes with Point- and Axis-Chiral Ligands Dependent on Coordination Structures

Takashi Harada, Yoko Nakano, Michiya Fujiki, Masanobu Naito, Tsuyoshi Kawai,* and Yasuchika Hasegawa*

Graduate School of Materials Science, Nara Institute of Science and Technology, 8916-5 Takayama-Cho, Ikoma, Nara 630-0192, Japan

Received August 19, 2009

Circularly polarized luminescence (CPL) of Eu(III) complexes with point- and axis-chiral ligands, [Eu((*R*/*S*)-BINAPO)(*D*-facam)$_3$] ((*R*/*S*)-BINAPO, (*R*/*S*)-2,2′-bis(diphenylphosphoryl)-1,1′-binaphthyl; *D*-facam, 3-trifluoroacetyl-*d*-camphor), [Eu(BIPHEPO)(*D*-facam)$_3$] (BIPHEPO, 2,2′-bis(diphenylphosphoryl)-biphenyl), [Eu(TPPO)$_2$(*D*-facam)$_3$] (TPPO, triphenylphosphine oxide), and [Eu((*R*)-BINAPO)(hfa)$_3$] (hfa, 1,1,1,5,5,5-hexafluoropentane-2,4-dione) are reported. The photophysical properties of chiral Eu(III) complexes were characterized by circular dichroism spectra, emission spectra, emission quantum yields, emission lifetimes, and CPL spectra. The dissymmetry factors of their CPL ($|g_{CPL}|$) at the magnetic-dipole transition of [Eu((*R*)-BINAPO)(*D*-facam)$_3$], [Eu((*S*)-BINAPO)(*D*-facam)$_3$], [Eu(BIPHEPO)(*D*-facam)$_3$], and [Eu(TPPO)$_2$(*D*-facam)$_3$] were as high as 0.44, 0.34, 0.24, and 0.47, respectively, while [Eu((*R*)-BINAPO)(hfa)$_3$] exhibited a relatively smaller dissymmetry factor ($|g_{CPL}|$=0.03). Their coordination structures were determined by the X-ray single-crystal analyses with shape-measure estimations. The photophysical relationship between the CPL properties and the electric transition probabilities of the chiral Eu(III) complexes is elucidated in terms of the coordination structures.

Introduction

Enantiopure luminescent metal complexes with chiral organic ligands have been a subject of great interest as attractive luminescent materials because of their unique luminescent properties, such as circularly polarized luminescence (CPL).[1] The characteristic CPL properties of the metal complexes come from chiral coordination structures. CPL properties of complexes of transition metal ions such as iridium(III), ruthenium(II), zinc(II), and copper(I) complexes with chiral coordination structures have been reported.[2−4] The magnitude of luminescent dissymmetry in the CPL properties is given by the dissymmetry factor g_{CPL}, as follows:

$$g_{(i\rightarrow j)} = 4\frac{|M_{ji}|}{|P_{ij}|}\cos\tau_{ij} \qquad (1)$$

where M_{ij}, P_{ij}, and τ_{ij} are the magnetic-dipole transition moments, the electric-dipole transition moments, and the angle between M_{ji} and P_{ij}, in the transition between i and j states, respectively.[5] The large g_{CPL} values in the CPL properties are expected in the band of the magnetic-dipole allowed transition and the electric-dipole forbidden transition. Such characteristic transitions are achieved in the magnetic-dipole transition of lanthanide(III) complexes. Indeed, the CPL properties of the magnetic-dipole transition in

*To whom correspondence should be addressed. Tel.: +81-743-72-6170 (T.K.), +81-743-72-6171 (Y.H.). Fax: +81-743-72-6170 (T.K.), +81-743-72-6171 (Y.H.). E-mail: tkawai@ms.naist.jp (T.K.), hasegawa@ms.naist.jp (Y.H.).

(1) (a) Richardson, F. S.; Riehl, J. P. *Chem. Rev.* **1977**, *77*, 773–792. (b) Riehl, J. P.; Richardson, F. S. *Chem. Rev.* **1986**, *86*, 1–15.
(2) Schaffner-Hamann, C.; von Zelewsky, A.; Barbieri, A.; Barigelletti, F.; Muller, G.; Riehl, J. P.; Neels, A. *J. Am. Chem. Soc.* **2004**, *126*, 9339–9348.
(3) Oyler, K. D.; Coughlin, F. J.; Bernhard, S. *J. Am. Chem. Soc.* **2007**, *129*, 210–217.
(4) Meskers, S. C. J.; Dekkers, H. P. J. M.; Rapenne, G.; Sauvage, J. P. *Chem.—Eur. J.* **2000**, *6*, 2129–2134.
(5) Richardson, F. S. *Inorg. Chem.* **1980**, *19*, 2806–2812.
(6) (a) Richardson, F. S. *Chem. Rev.* **1982**, *82*, 541–552. (b) Tsukube, H.; Shinoda, S. *Chem. Rev.* **2002**, *102*, 2389–2403. (c) Riehl, J. P.; Muller, G. Circulaly Polarized Luminescence Spectroscopy from Lanthanide Systems. In *Handbook on the Physics and Chemistry of Rare Earths*; Gschneidner, K. A., Bünzli, J. C. G., Pechcharsky, V. K., Eds.; North Holland Publishing Company: Amsterdam, 2005; Vol. *34*, Chapter 220, pp 289−357. (d) Bünzli, J. C. G.; Piguet, C. *Chem. Soc. Rev.* **2005**, *34*, 1048–1077. (e) Brittain, H. G.; Richardson, F. S. *J. Am. Chem. Soc.* **1976**, *98*, 5858–5863. (f) Brittain, H.; Richardson, F. S. *J. Am. Chem. Soc.* **1977**, *99*, 65–70. (g) Brittain, H. G.; Pearson, K. H. *Inorg. Chem.* **1983**, *22*, 78–82. (h) Maupin, C. L.; Dickins, R. S.; Govenlock, L. G.; Mathieu, C. E.; Parker, D.; Gareth Williams, J. A.; Riehl, J. P. *J. Phys. Chem. A* **2000**, *104*, 6709–6714. (i) Cantuel, M.; Bernaldielli, G.; Muller, G.; Riehl, J. P.; Piguet, C. *Inorg. Chem.* **2004**, *43*, 1840–1849. (j) Yu, J.; Parker, D.; Pal, R.; Poole, R. A.; Cann, M. J. *J. Am. Chem. Soc.* **2006**, *128*, 2294–2299. (k) Lama, M.; Mamula, O.; Kottas, G. S.; Rizzo, F.; De Cola, L.; Nakamura, A.; Kuroda, R.; Stoeckli-Evans, H. *Chem.—Eur. J.* **2007**, *13*, 7358–7373. (l) Bonsall, S. D.; Houcheime, M.; Straus, D. A.; Muller, G. *Chem. Commun.* **2007**, *35*, 3676–3678. (m) Leonard, J. P.; Jensen, P.; McCabe, T.; O'Brien, J. E.; Peacock, R. D.; Kruger, P. E.; Gunnlaugsson, T. *J. Am. Chem. Soc.* **2007**, *129*, 10986–10987. (n) Hopkins, T. A.; Metcalf, D. H.; Richardson, F. S. *Chirality* **2008**, *20*, 511–523. (o) Gregoliński, J.; Starynowicz, P.; Hua, K. T.; Lunkley, J. L.; Muller, G.; Lisowski, J. *J. Am. Chem. Soc.* **2008**, *130*, 17761–17773.

Published on Web 10/27/2009

Eu(III) complexes ($^5D_0 \rightarrow {}^7F_1$: 595 nm) have recently been extensively studied.[6] Parker and co-workers have reported the CPL properties of the lanthanide(III) complexes with point-chiral organic ligands, tetraazacyclododecane derivatives.[7] Raymond and co-workers have also described Eu(III) complexes as containing four point-chiral parts showing large g_{CPL} values (0.30) at the magnetic-dipole transition.[8] Recently, Kaizaki et al. have reported the remarkably large g_{CPL} of the magnetic-dipole transition in Eu(III) complexes with chiral camphor-derivative ligands.[9] However, their detailed characterization, such as crystallographic analysis, emission quantum yield, and emission lifetime has not yet been studied. Development of lanthanide(III) complexes with simultaneous intensive emission properties and larger optical dissymmetry is still desired. From the viewpoint of the intensive emission, the authors have previously reported on the enhanced emission of the Eu(III) complexes with β-diketonate and phosphine oxide ligands.[10] The enhanced emission was attributed to both suppressed vibronic quenching and enhanced emission probability.[10] Recently, the effect on the lanthanide−X vibrations has also been reported.[11] The former mainly originates from the specific nature of ligands with low-vibrational frequency (LVF) modes, while the latter comes from the hindered symmetry of the coordination structure. The combination of β-diketonate and phosphine oxide ligands for Eu(III) complexes was effective even in demonstrating the probability of laser action of the Eu(III) complexes.[10b,12] One may thus expect improved dissymmetry and intensity in light emission for Eu(III) complexes with phosphine oxides and β-diketonate camphor derivatives with appropriate chirality.

One of the authors has studied the optical chirality of lanthanide(III) complexes with chiral phosphine oxide and β-diketonate ligands and significantly large dissymmetry in circular dichroism (CD) spectra.[13] So far, however, no study on CPL activity of lanthanide(III) complexes with phosphine oxide and camphor ligands has been reported. Here, we focus on Eu(III) complexes with β-diketonate camphor ligands and phosphine oxides of chiral and achiral structures. We report on novel Eu(III) complexes with point- and axis-chiral ligands, [Eu((*R*/*S*)-BINAPO)(*D*-facam)$_3$] ((*R*/*S*)-BINAPO, (*R*/*S*)-2,2′-bis(diphenylphosphoryl)-1,1′-binaphthyl; *D*-facam, 3-trifluoroacetyl-*d*-camphor), [Eu(BIPHEPO)(*D*-facam)$_3$] (BIPHEPO, 2,2′-bis(diphenylphosphoryl)-1,1′-binaphthyl), [Eu(TPPO)$_2$(*D*-facam)$_3$] (TPPO, triphenylphosphine oxide), and Eu(III) complex with chiral (*R*)-BINAPO and achiral β-diketonato ligands (hfa, 1,1,1,5,5,5-hexafluoropentane-2,4-dione), [Eu((*R*)-BINAPO)(hfa)$_3$], whose chemical structures are illustrated in Figure 1. The phosphine oxide ligands, such as (*R*)-BINAPO, BIPHEPO, and TPPO show promise toward the development of enhanced electric-dipole transition probability by constructing asymmetric coordination structures.[10] The combination of phosphine oxide ligands and chiral β-diketonato ligands (*D*-facam) is also expected to produce a specific enantiomeric environment in the coordination sphere of the Eu(III) center. In the present study, we chose the *D*-facam ligand as the typical and commercially available chiral β-diketonate ligand which has been used for chiral Pr(III) and La(III) complexes.[14] The emission and CPL properties of chiral Eu(III) complexes with *D*-facam and phosphine oxide ligands are discussed in terms of the electric-dipole transition probability and geometrical coordination structures.

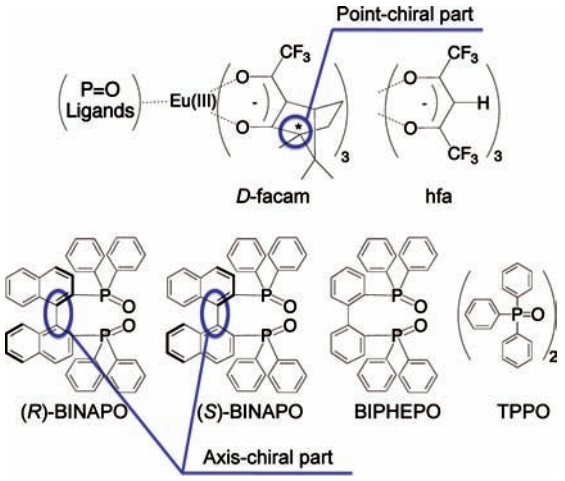

Figure 1. Chemical structures of chiral Eu(III) complexes.

Experimental Section

Apparatus. ^{1}H NMR, ^{19}F NMR, and ^{31}P NMR were obtained with JEOL AL-300 and JEOL ECP-500 spectrometers. ^{19}F NMR chemical shifts were determined with hexafluorobenzene as an internal standard ($\delta = -162.0$ ppm). ^{31}P NMR chemical shifts were determined with 85% H_3PO_4 as an external standard ($\delta = 0$ ppm). Matrix-assisted laser desorption ionization−time-of-flight mass spectrometry (MALDI-TOF MS) was performed using a DE-STR Voyager MALDI-TOF mass spectrometer. Electron ionization mass spectrometry (EI-MS), electrospray ionization mass spectrometry (ESI-MS), and fast atom bombardment mass spectrometry (FAB-MS) were recorded with a JEOL JMS-700 mass spectrometer. Infrared spectra were obtained recorded with a JASCO FT/IR-4200 spectrometer. Elemental analyses were performed with a Perkin-Elmer 2400 II.

Materials. (*R*/*S*)-1,1′-Bis(diphenylphosphino)-2,2′-binaphthyl ((*R*/*S*)-BINAP) and 1,1′-bis(diphenylphosphino)-biphenyl

(7) Dickins, R. S.; Howard, J. A. K.; Maupin, C. L.; Moloney, J. M.; Parker, D.; Riehl, J. P.; Siligardi, G.; Williams, J. A. *Chem.—Eur. J.* **1999**, *5*, 1095–1105. (b) Parker, D.; Dickins, R. S.; Puschmann, H.; Crossland, C.; Howard, J. A. *Chem. Rev.* **2002**, *102*, 1977–2010.

(8) (a) Petoud, S.; Muller, G.; Moore, E. G.; Xu, J.; Sokolniski, J.; Riehl, J. P.; Le, U. N.; Cohen, S. M.; Raymond, K. N. *J. Am. Chem. Soc.* **2007**, *129*, 77–83. (b) Seitz, M.; Moore, E. G.; Ingram, A. J.; Muller, G.; Raymond, K. Y. *J. Am. Chem. Soc.* **2007**, *129*, 15468–15470.

(9) (a) Lunkley, J. L.; Shirotani, D.; Yamanari, K.; Kaizaki, S.; Muller, G. *J. Am. Chem. Soc.* **2008**, *130*, 13814–13815. (b) Shirotani, D.; Suzuki, T.; Kaizaki, S. *Inorg. Chem.* **2006**, *45*, 6111–6113. (c) Shirotani, D.; Suzuki, T.; Yamanari, K.; Kaizaki, S. *J. Alloys Compd.* **2008**, *451*, 325–328.

(10) (a) Hasegawa, Y.; Kimura, Y.; Murakoshi, K.; Wada, Y.; Yamanaka, T.; Kim, J.; Nakashima, N.; Yanagida, S. *J. Phys. Chem.* **1996**, *100*, 10201–10205. (b) Hasegawa, Y.; Murakoshi, K.; Wada, Y.; Yanagida, S.; Kim, J.; Nakashima, N.; Yamanaka, T. *Chem. Phys. Lett.* **1996**, *248*, 8–12. (c) Hasegawa, Y.; Yamamuro, M.; Wada, Y.; Kanehisa, N.; Kai, Y.; Yanagida, S. *J. Phys. Chem. A* **2003**, *107*, 1697–1702. (d) Nakamura, K.; Hasegawa, Y.; Kawai, H.; Yasuda, N.; Kanehisa, N.; Kai, Y.; Nagamura, T.; Yanagida, S.; Wada, Y. *J. Phys. Chem. A* **2007**, *111*, 3029–3037. (e) Hasegawa, Y.; Tsuruoka, S.; Yoshida, T.; Kawai, H.; Kawai, T. *J. Phys. Chem. A* **2008**, *112*, 803–807.

(11) Norton, K.; Kumar, G. A.; Dilks, J. L.; Emge, T. J.; Riman, R. E.; Brik, M. G.; Brennan, J. G. *Inorg. Chem.* **2009**, *48*, 3573–3580.

(12) Hasegawa, Y.; Wada, Y.; Yanagida, S.; Kawai, H.; Yasuda, N.; Nagamura, N. *Appl. Phys. Lett.* **2003**, *83*, 3599–3601.

(13) Subhan, M. A.; Hasegawa, Y.; Suzuki, T.; Kaizaki, S.; Yanagida, S. *Inorg. Chim. Acta* **2009**, *362*, 136–142.

(14) Cunningham, J. A.; Sievers, R. E. *J. Am. Chem. Soc.* **1975**, *97*, 1586–1588. (b) Shirotani, D.; Suzuki, T.; Kaizaki, S. *Inorg. Chem.* **2006**, *45*, 6111–6113. (c) Shirotani, D.; Suzuki, T.; Yamanari, K.; Kaizaki, S. *J. Alloys Compd.* **2008**, *451*, 325–328.

(BIPHEP) were purchased from Tokyo Chemical Industry Co., Ltd. Europium(III) acetate tetrahydrate (99.9%) and acetone-d_6 (99.9%) were obtained from Wako Pure Chemical Industries, Ltd. TPPO, 1,1,1,5,5,5-hexafluoropentane-2,4-dione (hfa), and tris(3-trifluoroacetyl-*d*-camphorato)europium(III) ([Eu(*D*-facam)$_3$], purity > 97%) were purchased from Aldrich Chemical Co., Inc. All other organic compounds were reagent grade and used as received.

Preparation of (*R*/*S*)-2,2′-Bis(diphenylphosphoryl)-1,1′-binaphthyl ((*R*/*S*)-BINAPO). (*R*/*S*)-BINAPO was prepared by the oxidation of (*R*/*S*)-BINAP.[15] (*R*/*S*)-BINAP (3.0 g, 4.6 mmol) was dissolved in dichloromethane (200 mL) and stirred at 0 °C for 1 h. A 30% hydrogen peroxide solution (10 mL) was added dropwise to the above solution. The solution was stirred for 12 h, and distilled water (100 mL) was added into the solution. The solution was extracted by dichloromethane (50 mL, 3 times). Magnesium sulfate dehydrate was added to the organic phases for dehydration. After filtration, the organic phase was evaporated using a rotary evaporator, which gave white solids. Recrystallization with hot methanol/water solution gave colorless needle crystals.

(*R*)-BINAPO. Yield: 88%. MALDI-TOF MS (positive): *m*/*z* 655.194 ([M + H]$^+$). ^{1}H NMR ($CDCl_3$, 500 MHz, 298 K): δ 7.85−7.80 (q, 4H), 7.71−7.67 (q, 4H), 7.45−7.33 (m, 12H), 7.25−7.22 (m, 8H), 6.80−6.79 (d, 4H). ^{31}P NMR ($CDCl_3$, 200 MHz, 298 K): δ 28.83. Anal. Found: C, 76.84%; H, 4.91%. Calcd for $C_{44}H_{32}O_2P_2 \cdot MeOH \cdot H_2O$: C, 76.69%; H, 5.01%.

(*S*)-BINAPO. Yield: 92%. ESI-MS (positive): *m*/*z* 655.196 ([M + H]$^+$), 1331.365 ([2M + Na]$^+$). ^{1}H NMR ($CDCl_3$, 500 MHz, 298 K): δ 7.85−7.80 (q, 4H), 7.70−7.67 (q, 4H), 7.45−7.33 (m, 12H), 7.27−7.22 (m, 8H), 6.76−6.75 (d, 4H). ^{31}P NMR ($CDCl_3$, 200 MHz, 298 K): δ 29.18. Anal. Found: C, 77.04%; H, 5.20%. Calcd for $C_{44}H_{32}O_2P_2 \cdot MeOH \cdot H_2O$: C, 76.69%; H, 5.01%.

Preparation of 2,2′-Bis(diphenylphosphoryl)-biphenyl (BIPHEPO). BIPHEPO was synthesized in the preparation of (*R*/*S*)-BINAPO, according to the procedure described in the literature.[15] Recrystallization of methanol/water gave white rhombic crystals. Yield: 85%. EI-MS (positive): *m*/*z* 553.148 ([M − H]$^+$). ^{1}H NMR ($CDCl_3$, 500 MHz, 298 K): δ 7.73−7.69 (t, 4H), 7.66−7.63 (t, 4H), 7.53−7.50 (t, 2H), 7.47−7.43 (t, 4H), 7.36−7.33 (t, 2H), 7.31−7.28 (t, 4H), 7.20−7.15 (m, 6H), 7.0 (t, 2H). ^{31}P NMR ($CDCl_3$, 200 MHz, 298 K): δ 28.77. Anal. Found: C, 75.88%; H, 4.90%. Calcd for $C_{36}H_{28}O_2P_2 \cdot 0.8H_2O$: C, 75.99%; H, 5.24%.

Preparation of Tris(hexafluoroacetylacetonato)europium(III) ([Eu(hfa)$_3$(H_2O)$_2$]). [Eu(hfa)$_3$(H_2O)$_2$] was prepared with the procedure described in the previous report.[12] Yield: 78%. ^{19}F NMR (CD_3COCD_3, 500 MHz, 298 K): δ −80.54 (s, C−F). Anal. Found: C, 22.02%; H, 1.19%. Calcd for $EuC_{15}H_7O_8F_{18} \cdot H_2O$: C, 21.78%; H, 1.10%.

Preparation of Tris(3-trifluoroacetyl-*d*-camphorato)europium(III)((*R*/*S*)-2,2′-bis(diphenylphosphoryl)-1,1′-binaphthyl) ([Eu((*R*/*S*)-BINAPO)(*D*-facam)$_3$]). [Eu(*D*-facam)$_3$] (0.50 g, 0.54 mmol) and (*R*/*S*)-BINAPO (0.35 g, 0.54 mmol) were dissolved in methanol (60 mL) and refluxed under stirring for 12 h. The reaction solution was evaporated using a rotary evaporator. The obtained powder was recrystallized using a chloroform/*n*-hexane solution, which gave yellow needle crystals.

[Eu((*R*)-BINAPO)(*D*-facam)$_3$]. Yield: 63%. ESI-MS (positive): *m*/*z* 1299.297 ([M − (*D*-facam)]$^+$). ^{1}H NMR ($CDCl_3$, 300 MHz, 298 K): δ 10.1−7.3, 7.2−6.2 (m, aromatic), 2.4 (s), 2.0 (t), 1.0 (t), 0.3 (t), 0.2 (s), −0.2 (s), −0.7 (s). ^{31}P NMR ($CDCl_3$, 200 MHz, 298 K): δ −50.17. FT-IR (ATR): 3800−3500 (w, O−H), 3050, 3000−2800 (w, C−H), 1655 (s, C═O), 1540 (s), 1440 (s), 1250−1050 (s, C−F), 1180 (s, P═O), 690 (s, aromatic) cm^{-1}. Anal. Found: C, 61.02%; H, 4.89%. Calcd for $EuC_{80}H_{74}O_8F_9P_2 \cdot H_2O$: C, 61.35; H, 4.89%.

[Eu((*S*)-BINAPO)(*D*-facam)$_3$]. Yield: 66%. ESI-MS (positive): *m*/*z* 1299.297 ([M − (*D*-facam)]$^+$). ^{1}H NMR ($CDCl_3$, 300 MHz, 298 K): δ 8.93 (s), 8.73−8.70 (d), 8.55 (s), 7.98−7.92 (t), 7.86−7.77 (q), 7.48−7.44 (t), 7.35 (s), 6.69 (s), 6.55 (s), 6.16 (s), 3.17 (s), 1.36 (s), 1.26−1.23 (m), 1.15−1.05 (q), 0.63−0.49 (m), −0.86 (s), −1.48 to −1.51 (t). ^{31}P NMR ($CDCl_3$, 200 MHz, 298 K): δ −58.74. FT-IR (KBr): 3800−3500 (w, O−H), 3060, 3030−2780 (w, C−H), 1660 (s, C═O), 1540 (s), 1440 (s), 1250−1050 (s, C−F), 1180 (s, P═O), 690 (s, aromatic) cm^{-1}. Anal. Found: C, 61.90%; H, 4.66%. Calcd for $EuC_{80}H_{74}O_8F_9P_2$: C, 62.06%; H, 4.82%.

Preparation of Tris(3-trifluoroacetyl-*d*-camphorato)europium(III) (2,2′-Bis(diphenylphosphoryl)-biphenyl) ([Eu(BIPHEPO)(*D*-facam)$_3$]). [Eu(BIPHEPO)(*D*-facam)$_3$] was prepared in the same was as given in the synthesis of [Eu((*R*/*S*)-BINAPO)(*D*-facam)$_3$], using BIPHEPO (0.30 g, 0.54 mmol) instead of (*R*/*S*)-BINAPO in methanol. The reaction solution was left at rest. The white precipitate was removed by the filtration. The obtained powder was recrystallized from hot acetonitrile, which gave white crystals. Yield: 59%. ESI-MS (positive): *m*/*z* 1199.266 ([M − (*D*-facam)]$^+$). ^{1}H NMR ($CDCl_3$, 300 MHz, 298K): δ 10.16 (s), 9.88 (s), 9.44 (s), 8.61−8.55 (d), 8.25 (s), 7.86−7.58 (d), 7.11 (s), 6.58 (s), 4.12 (s), 3.15 (s), 2.82−2.67 (d), 2.26 (s), 2.01 (s), 1.37 (s), 1.11−0.94 (q), 0.54 (s), 0.34 (s), 0.24 (s), 0.07 (s), −0.08 (s), −0.43 (s), −0.67 (s), −1.28 (s), −1.67 (s), −1.81 (s). ^{31}P NMR ($CDCl_3$, 200 MHz, 298 K): δ −57.28, −62.66. FT-IR (ATR): 3850−3495 (w, O−H), 3060, 3020−2780 (w, C−H), 1670 (s, C═O), 1540 (s), 1440 (s), 1260−1050 (s, C−F), 1180 (s, P═O), 690 (s, aromatic) cm^{-1}. Anal. Found: C, 58.57%; H, 4.61%. Calcd for $EuC_{72}H_{70}O_8F_9P_2 \cdot 2MeOH$: C, 58.77%; H, 4.80%.

Preparation of Tris(3-trifluoroacetyl-*d*-camphorato)europium(III) Bis(triphenylphosphine oxide) ([Eu(TPPO)$_2$(*D*-facam)$_3$]). [Eu(TPPO)$_2$(*D*-facam)$_3$] was prepared in the same was as given in as the synthesis of [Eu((*R*/*S*)-BINAPO)(*D*-facam)$_3$], using TPPO (0.25 g, 0.54 mmol) instead of (*R*/*S*)-BINAPO. TPPO was purchased and used after crystallization using a hot methanol/water solution. The reaction solution was evaporated using a rotary evaporator. The obtained powder was recrystallized from a hot acetonitrile solution and gave yellow-white needle crystals. Yield: 56%. ESI-MS (positive): *m*/*z* 1203.218 ([M − (*D*-facam)]$^+$). ^{1}H NMR ($CDCl_3$, 300 MHz, 298K): δ 11.99 (s), 7.78 (s), 3.39 (s), 2.52 (s), 1.42 (s), 0.85 (s), −0.08 (s), −0.83 (s), −1.47 (s). FT-IR (KBr): 3950−3550 (w, br, O−H), 3060 (s, C−H), 3025−2825 (s, C−H), 1965 (m), 1910 (m), 1825 (m), 1660 (s, C═O), 1540 (s), 1439 (s), 1200 (s, P═O) 1180−1050 (s, C−F), 725 (s, aromatic), 695 (s, aromatic) cm^{-1}. Anal. Found: C, 59.33%; H, 4.70%. Calcd for $EuC_{72}H_{72}O_8F_9P_2$: C, 59.63%; H, 5.00%.

Preparation of Tris(hexafluoroacetylacetonato)europium(III)-((*R*)-2,2′-bis(diphenylphosphoryl)-1,1′-binaphthyl) ([Eu((*R*)-BINAPO)(hfa)$_3$]). [Eu((*R*)-BINAPO)(hfa)$_3$] was prepared with the procedure described in the previous report.[16] Yield: 40%. FAB-MS (positive): *m*/*z* 1222.087 ([M − (hfa)]$^+$). ^{1}H NMR (acetone-d_6, 300 MHz, 298 K): δ 8.27−6.46 (m, aromatic), 5.86−5.72 (s). IR (ATR): 3800−3550 (w, O−H), 3060 (w, C−H), 1650 (s, C═O), 1600−1460 (m, br), 1440 (s), 1250−1050 (s, C−F), 1200 (s, P═O), 690 (s, aromatic) cm^{-1}. Anal. Found: C, 49.62; H, 2.52%. Calcd for $EuC_{59}H_{35}O_8F_{18}P_2$: C, 49.61; H, 2.45%.

Optical Measurements. Measurement of absorption and CD spectra were performed at room temperature with JASCO V-660, JASCO J-725, and JASCO J-820 machines. An acetone-d_6 solution (1.0 mM) of the Eu(III) complexes in quartz cells

(15) Merthod, M.; Saluzzo, C.; Mignani, G.; Lemaire, M. *Tetrahedron: Asymmetry* **2004**, *15*, 639–645.

(16) Harada, T.; Hasegawa, Y.; Nakano, Y.; Fujiki, M.; Naito, M.; Wada, T.; Inoue, Y.; Kawai, T. *J. Alloys Compd.* In press.

were degassed with bubbling N_2 for measurements of emission spectra, emission quantum yields, emission lifetimes, and CPL spectra. The emission spectra were measured at room temperature using JASCO FP-6500; HITACHI F-4500; and ACTON SpectraPro 2300i systems with a CCD detector, the Roper PIXIS 100. The spectra were corrected for detector sensitivity and lamp intensity variations. The emission quantum yields excited at 465 nm were estimated by comparing the integral emission intensity and absorbance at the excitation wavelength with those of the [Eu(BIPHEPO)$(hfa)_3$] solution (dissolved in acetone-d_6, 0.05 M, $\Phi = 0.60$) as a reference.[17] In the emission lifetime measurements, the samples were excited by a N_2 laser (Usho KEC-160; wavelength, 337 nm; pulse width, 600 ps; 10 Hz). The emission profiles were recorded using a streak camera (Hamamatsu, picosecond fluorescence measurement system, C4780). The CPL spectra measurements were performed with a JASCO CPL-200 spectrometer. The dissymmetry factors of CPL spectra, g_{CPL}, were corrected by the instrumental correction function of the CPL spectrometer.

Crystallography. Colorless single crystals of [Eu$(TPPO)_2$-$(D$-facam$)_3$] and [Eu(BIPHEPO)$(D$-facam$)_3$] were mounted on a glass fiber with epoxy resin. X-ray diffraction intensity was collected with a Rigaku RAXIS RAPID (3 kW) imaging plate area detector with graphite monochromated Mo Kα radiation in the ω-2θ scanning mode at 193 ± 1 K. Non-hydrogen atoms were refined anisotropically. Hydrogen atoms were placed in calculated positions (C−H, 0.95 Å) and not refined. All calculations were performed with the Rigaku CrystalStructure 3.8.1 software. On the basis of previous X-ray analyses, the analyses using CF_3 conformations in Eu(III) complexes were carried out.[9b]

Results and Discussions

Absorption and Circular Dichroism (CD) Spectra. The absorption and CD spectra of Eu(III) complexes with chiral ligands, [Eu((R/S)-BINAPO)$(D$-facam$)_3$], [Eu(BIPHEPO)$(D$-facam$)_3$], [Eu$(TPPO)_2(D$-facam$)_3$], and [Eu-$((R)$-BINAPO)$(hfa)_3$], are shown in Figure 2. The large absorption bands in UV regions are assigned to the $\pi-\pi^*$ transition of phosphine ligands ((R/S)-BINAPO, BIPHEPO, and TPPO) and β-diketonato ligands (D-facam and hfa). The absorption bands at around 300−320 nm and ∼240 nm dominantly originate from D-facam and the phosphine oxide ligand, respectively. Weak absorption bands at 465 and 525 nm (Figure 2a, inset) are attributed to the $^7F_0 \rightarrow {}^5D_2$ and $^7F_0 \rightarrow {}^5D_1$ transitions in Eu(III) ions. The molar absorption coefficients at 465 and 530 nm were about 1.5 and 0.30 $M^{-1}cm^{-1}$, respectively.

In the measurements of CD spectra, the two enantiomeric (R)-BINAPO and (S)-BINAPO molecules gave mirror images, as shown in Figure S1 in the Supporting Information. The two diastereomeric complexes Eu((R)-BINAPO)$(D$-facam$)_3$] and [Eu((S)-BINAPO)$(D$-facam$)_3$] exhibited characteristic CD activity, as shown in Figure 2a. They have almost symmetric CD profiles, both with wavelength ranges between 200 and 260 nm, which correspond to the phosphine oxide ligands. Those in the longer wavelength range, meanwhile, are not symmetric but are both positive, which suggests contribution of D-facam ligands. All Eu(III) complexes with D-facam ligands showed a positive CD signal in the wavelength range around 280−350 nm. The CD spectra of [Eu(BIPHEPO)$(D$-facam$)_3$] and [Eu$(TPPO)_2(D$-facam$)_3$] presented in Figure 2b exhibited a characteristic peak at 305 nm which roughly agreed with that observed in [Eu((S)-BINAPO)$(D$-facam$)_3$]. Since CD spectra of [Eu(BIPHEPO)$(D$-facam$)_3$] and [Eu$(TPPO)_2(D$-facam$)_3$] almost coincide with each other, their CD spectra could be assigned to the D-facam ligands. We thus compared the CD spectrum of [Eu((S)-BINAPO)$(D$-facam$)_3$] with the sum of CD spectra of the (S)-BINAPO ligand and [Eu$(TPPO)_2(D$-facam$)_3$] and confirmed their agreement, as shown in Figure S2 in the Supporting Information. A rather complicated CD spectrum of [Eu((R)-BINAPO)-$(D$-facam$)_3$] was also reproduced by summation of those of (R)-BINAPO and [Eu$(TPPO)_2(D$-facam$)_3$], as also summarized in Figure S2. These results indicate that the structures and thus optical chirality of the D-facam and the (R)- and (S)-BINAPO are almost maintained in these complexes.

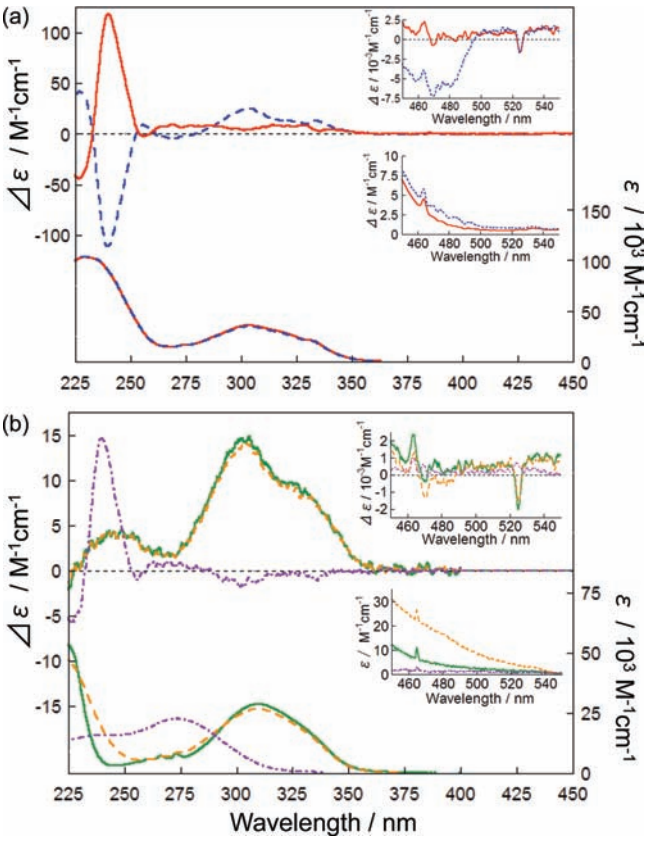

Figure 2. (a) Absorption (under) and CD (upper) spectra of [Eu((R)-BINAPO)$(D$-facam$)_3$] (red, solid line) and [Eu((S)-BINAPO)$(D$-facam$)_3$] (blue, dashed line). ([Eu((R)-BINAPO)$(D$-facam$)_3$], 4.9×10^{-5} M; [Eu((S)-BINAPO)$(D$-facam$)_3$], 5.1×10^{-5} M; in methanol; optical path length, 1.0 mm. Inset: Absorption and CD spectra at the absorption bands from the 4f−4f transitions of Eu(III) ions: 5.0×10^{-3} M; in methanol; optical path length, 10.0 mm. (b) Absorption (under) and CD (upper) spectra of [Eu(BIPHEPO)$(D$-facam$)_3$] (orange, dashed line), [Eu$(TPPO)_2(D$-facam$)_3$] (green, solid line), and [Eu((R)-BINAPO)$(hfa)_3$] (purple, chain line). [Eu(BIPHEPO)$(D$-facam$)_3$], 7.2×10^{-5} M; [Eu$(TPPO)_2(D$-facam$)_3$], 5.1×10^{-5} M; [Eu((R)-BINAPO)-$(hfa)_3$], 9.8×10^{-4} M; in methanol; optical path length, 1.0 mm. Inset: Absorption and CD spectra at the absorption bands from the 4f−4f transitions of Eu(III) ions: 5.0×10^{-3} M; in methanol; optical path length, 10.0 mm.

(17) Nakamura, K.; Hasegawa, Y.; Kawai, H.; Yasuda, N.; Tsukahara, Y.; Wada, Y. *Thin Solid Films* **2008**, *516*, 2376–2381.

Here, we estimated the dissymmetry factors (g_{CD}) of the CD spectra as follows:

$$g_{CD} = \frac{\Delta\varepsilon}{\frac{1}{2}\varepsilon} = \frac{(\varepsilon_L - \varepsilon_R)}{\frac{1}{2}(\varepsilon_L + \varepsilon_R)} \quad (2)$$

where, ε_L and ε_R are the molar absorption coefficients for the left and right circularly polarized light, respectively. The g_{CD} at the $\pi-\pi^*$ transition of [Eu((*R*/*S*)-BINAPO)(*D*-facam)$_3$] ($|g_{CD}| = 1.3 \times 10^{-3}$, at 240 nm) is almost the same as those of corresponding (*R*/*S*)-BINAPO molecules ($|g_{CD}| = 1.3 \times 10^{-3}$). These results also suggest that the conformational structures of free (*R*/*S*)-BINAPO molecules might be similar to those in [Eu((*R*/*S*)-BINAPO)(*D*-facam)$_3$] in methanol.[18] The g_{CD} values of the [Eu((*R*)-BINAPO)(*D*-facam)$_3$], [Eu(BIPHEPO)(*D*-facam)$_3$], and [Eu(TPPO)$_2$(*D*-facam)$_3$] at around 304 nm were found to be 1.2×10^{-4}, 5.4×10^{-4}, and 5.2×10^{-4}, respectively. The relatively small g_{CD} of [Eu((*R*)-BINAPO)(*D*-facam)$_3$] is also attributed to opposite g_{CD} values of *D*-facam and (*R*)-BINAPO ligands.

Weak CD bands were also observed at 465 and 525 nm, corresponding to the absorption bands of the 4f−4f transitions in Eu(III) ions (Figure 2b, inset), and their values were estimated to be approximately 1.0×10^{-3} and 1.0×10^{-2}, respectively. It should be noted that these values contain a considerably large probable error because of their extinction coefficients being as weak as 2.0 M^{-1} cm^{-1}. In order to discuss the optical chirality of the electronic transition of the Eu(III) center, the characterizations using the emission spectra and CPL spectra were, thus, expected to be effective.

Emission and CPL Spectra. The emission and CPL spectra of Eu(III) complexes in acetone-d_6 are shown in Figure 3. Five characteristic emission bands of Eu(III) were observed at 580, 593, 611, 650, and 700 nm, which were assigned to the 4f−4f transition bands, $^5D_0 \rightarrow {}^7F_J$ with $J = 0, 1, 2, 3,$ and 4, respectively. The emission spectra in Figure 3 were normalized with respect to the $^5D_0 \rightarrow {}^7F_1$ (magnetic-dipole) transition band, which is known to be insensitive to the surrounding environment of the Eu(III) ion.[10] The emission band at 611 nm, $^5D_0 \rightarrow {}^7F_2$, is due to the electric-dipole transition. Probability of $^5D_0 \rightarrow {}^7F_2$ transition considerably depends on the geometrical symmetry of the coordination structure and is enhanced in those of low symmetry.[19] In order to estimate the relative transition probability of the electric-dipole transition, we evaluated the relative integrated intensity of the $^5D_0 \rightarrow {}^7F_2$ transition with respect to that of the $^5D_0 \rightarrow {}^7F_1$ transition band ($A_{rel} = A_{ED}/A_{MD}$; A_{ED}, integrated intensity at the electric-dipole transition; A_{MD}, integrated intensity at the magnetic-dipole transition). The A_{rel} values in Eu(III) complexes are listed in Table 1. The A_{rel} values in the Eu(III) complexes with *D*-facam were considerably larger than that of the Eu(III) complex with hfa ligands. The introduction of chiral *D*-facam ligands would lead to effective reduction of the geometrical symmetry around the Eu(III) ion.

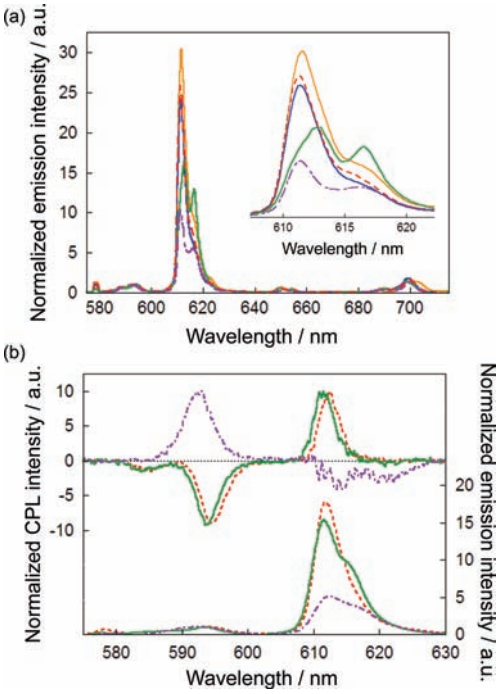

Figure 3. (a) Normalized emission spectra of [Eu(BIPHEPO)-(*D*-facam)$_3$] (orange, solid line), [Eu((*R*)-BINAPO)(*D*-facam)$_3$] (red, dashed line), [Eu((*S*)-BINAPO)(*D*-facam)$_3$] (blue, solid line), [Eu(TPPO)$_2$(*D*-facam)$_3$] (green, solid line), and [Eu((*R*)-BINAPO)(hfa)$_3$] (purple, chain line): 1.0×10^{-3} M; in acetone-d_6; optical path length, 10 mm. Inset: The $^5D_0 \rightarrow {}^7F_2$ (electric-dipole) transition. (b) Normalized emission (under) and normalized CPL (upper) spectra of [Eu((*R*)-BINAPO)(*D*-facam)$_3$] (red, dashed line), [Eu(TPPO)$_2$(*D*-facam)$_3$] (green, solid line), and [Eu((*R*)-BINAPO)(hfa)$_3$] (purple, chain line): 1.0×10^{-3} M; in acetone-d_6; optical path, 10.0 mm.

Table 1. Relative Integrated Emission Intensity (A_{rel}) and the Dissymmetry Factors of CPL Spectra (g_{CPL}) at the $^5D_0 \rightarrow {}^7F_1$ (Magnetic-Dipole) and $^5D_0 \rightarrow {}^7F_2$ (Electric-Dipole) Transitions

complex	A_{rel}	$\lvert g_{CPL}\rvert$ ($^5D_0 \rightarrow {}^7F_1$)	$\lvert g_{CPL}\rvert$ ($^5D_0 \rightarrow {}^7F_2$)
[Eu((*R*)-BINAPO) (*D*-facam)$_3$]	14	0.44 (594 nm)	0.029 (612.5 nm)
[Eu((*S*)-BINAPO) (*D*-facam)$_3$]	14	0.34 (595 nm)	0.024 (613 nm)
[Eu(BIPHEPO) (*D*-facam)$_3$]	16	0.24 (597 nm)	0.014 (614.5 nm)
[Eu(TPPO)$_2$ (*D*-facam)$_3$]	14	0.47 (594 nm)	0.033 (611.5 nm)
[Eu((*R*)-BINAPO) (hfa)$_3$]	8	0.03 (593 nm)	0.003 (614.5 nm)

The CPL spectra of chiral Eu(III) complexes in acetone-d_6 are shown in Figure 3b. The CPL signals are given by the difference between the left and right circularly polarized emission intensities ($I_{CPL} = I_L - I_R$). The emission and CPL spectra in Figure 3b were also normalized with respect to the $^5D_0 \rightarrow {}^7F_1$ (magnetic-dipole) transitions. CPL spectral shapes [Eu((*R*)-BINAPO)(*D*-facam)$_3$] and [Eu(TPPO)$_2$(*D*-facam)$_3$] were notably different from that of [Eu((*R*)-BINAPO)(hfa)$_3$]. These spectral differences might be caused by the difference in chiral coordination structures of Eu(III) complexes. We also found that the CPL spectra of [Eu((*S*)-BINAPO)-(*D*-facam)$_3$] and [Eu(BIPHEPO)(*D*-facam)$_3$] exhibited similar shapes to that of [Eu((*R*)-BINAPO)(*D*-facam)$_3$] (Supporting Information, Figure S3). The CPL spectral shapes of Eu(III) complexes with *D*-facam might, thus, be mainly induced by introducing *D*-facam ligands. In

(18) Hanazaki, I.; Akimoto, K. *J. Am. Chem. Soc.* **1975**, *97*, 1586–1588.
(19) (a) Lunstroot, K.; Driesen, K.; Nockemann, P.; Görller-Walrand, C.; Binnemans, K.; Bellayer, S.; Le Bideau, J.; Vioux, A. *Chem. Mater.* **2006**, *18*, 5711–5715. (b) Eliseeva, S. V.; Kotova, O. V.; Gumy, F.; Semenov, S. N.; Kessler, V. G.; Lepnev, L. S.; Bünzli, J. C. G.; Kuzmina, N. P. *J. Phys. Chem. A* **2008**, *112*, 3614–3626. (c) Nakagawa, T.; Hasegawa, Y.; Kawai, T. *J. Phys. Chem. A* **2008**, *112*, 5096–5103.

Table 2. Emission Quantum Yields and Emission Lifetimes of Chiral Eu(III) Complexes[a]

complex	$\Phi_{f\text{-}f}$/ %	τ/ms
[Eu((*R*)-BINAPO)(*D*-facam)$_3$]	1.8	0.091 (73%) 0.31 (27%)
[Eu((*S*)-BINAPO)(*D*-facam)$_3$]	1.5	0.11 (77%) 0.32 (23%)
[Eu(BIPHEPO)(*D*-facam)$_3$]	3.1	0.29 (65%) 0.96 (35%)
[Eu(TPPO)$_2$(*D*-facam)$_3$]	0.65	0.12
[Eu((*R*)-BINAPO)(hfa)$_3$]	53.0	2.1

[a] The emission quantum yields (Φ_{f-f}) of Eu(III) complexes in acetone-d_6 (1.0 mM) were measured by excitation at 465 nm ($^7F_0 \rightarrow {}^5D_2$). The emission lifetimes (τ) were measured by excitation at 337 nm.

contrast, [Eu((*R*)-BINAPO)(hfa)$_3$] showed CPL spectra of considerably different shapes compared to those of Eu(III) complexes with *D*-facam ligands.

The degree of the CPL is usually discussed in terms of the luminescent dissymmetry factor, g_{CPL}, which is defined as follows:

$$g_{CPL} = \frac{I_L - I_R}{\frac{1}{2}(I_L + I_R)} \quad (3)$$

where, I_L and I_R refer to the left and right circularly polarized emission intensities, respectively. The g_{CPL} values at the magnetic-dipole and the electric-dipole transitions of Eu(III) complexes are also summarized in Table 1. The g_{CPL} values at the magnetic-dipole transition were significantly larger than those at the electric-dipole transition in all complexes. The $|g_{CPL}|$ values of Eu(III) complexes with chiral *D*-facam were notably larger than those of [Eu((*R*)-BINAPO)(hfa)$_3$] with achiral hfa ligands. We also found that the g_{CPL} values depend on the structures of phosphine oxide ligands. [Eu(TPPO)$_2$-(*D*-facam)$_3$] showed the largest g_{CPL} value (0.47) among the present Eu(III) complexes. The g_{CPL} value of [Eu((*R*)-BINAPO)(*D*-facam)$_3$] was larger than that of [Eu((*S*)-BINAPO)(*D*-facam)$_3$]. These results indicate that the geometrical structure of [Eu((*R*)-BINAPO)(*D*-facam)$_3$] is different from that of [Eu((*S*)-BINAPO)(*D*-facam)$_3$].

Emission Quantum Yields and Emission Lifetimes. The emission quantum yields of Eu(III) complexes in acetone-d_6 are summarized in Table 2. The emission quantum yields of [Eu((*R*)-BINAPO)(hfa)$_3$] were much higher than those of Eu(III) complexes with *D*-facam. In the energy gap theory, the nonradiative transitions are effectively promoted by the organic ligands with a high-frequency vibrational mode.[11] We have previously reported on the effective suppression of nonradiative transition in lanthanide(III) complexes with hfa ligands that have C−F bonds composed of LVF.[20] The LVF ligands with C−F bonds instead of C−H bonds are effective in suppression of the nonradiative transition and enhancement of emission quantum yield. The remarkable emission quantum yield of [Eu((*R*)-BINAPO)(hfa)$_3$] might be due to effective suppression of the nonradiative transition via vibrational relaxation in Eu(III) complex.[16] According to the vibrational relaxation of lanthanide(III) complexes, Beeby et al. and Werts et al. have reported on the estimation using the emission spectrum and the observed lifetime.[21] On the basis of our emission quantum yields and lifetimes, we here estimated the nonradiative rate constants (k_{nr}) of [Eu(TPPO)$_2$(*D*-facam)$_3$] and [Eu(TPPO)$_2$(hfa)$_3$] to compare their nonradiative processes.[17] The k_{nr}'s of [Eu(TPPO)$_2$(*D*-facam)$_3$] and [Eu(TPPO)$_2$(hfa)$_3$] were found to be 8.3×10^{-3} and 4.7×10^{-2} s^{-1}, respectively. These results suggest that *D*-facam ligands promote the vibrational relaxation effectively. Relatively small emission quantum yields of chiral Eu(III) complexes with *D*-facam ligands could be attributed to the nonradiative transition via vibrational relaxation of high-vibrational C−H bonds in the *D*-facam ligand.

As also summarized in Table 2, the emission lifetimes of [Eu(TPPO)$_2$(*D*-facam)$_3$] and [Eu((*R*)-BINAPO)(hfa)$_3$] were determined from the slope of logarithmic plots of decay profiles to be 0.12 and 2.1 ms, respectively. We also observed that the emission decays of [Eu((*R*/*S*)-BINAPO)(*D*-facam)$_3$] and [Eu(BIPHEPO)(*D*-facam)$_3$] consist of two components, which suggests the presence of two luminescent species in acetone-d_6. The k_{nr} constants of [Eu((*R*/*S*)-BINAPO)(*D*-facam)$_3$] might be almost similar to those of [Eu(BIPHEPO)(*D*-facam)$_3$] because of the similar vibrational structures of their ligands. On the other hand, it is reported that Eu(III) complexes show large radiative rate constants (k_r) with the distorted coordination structures.[10c,d] We suggested that the two emission lifetime components observed in [Eu((*R*/*S*)-BINAPO)(*D*-facam)$_3$] and [Eu(BIPHEPO)-(*D*-facam)$_3$] are related to the difference of the distorted coordination structures of emission components. Lower-symmetric coordination structures in these Eu(III) complexes might promote shorter components in the emission lifetimes.

Coordination Structures. We carried out the X-ray crystallographic analyses of the chiral Eu(III) complexes. The ORTEP views of [Eu(TPPO)$_2$(*D*-facam)$_3$] and [Eu(BIPHEPO)(*D*-facam)$_3$] are shown in Figure 4 and Table 3. The coordination site of [Eu(TPPO)$_2$(*D*-facam)$_3$] consists of two TPPO and three *D*-facam ligands, which are tentatively assigned to *D*-facam 1, *D*-facam 2, and *D*-facam 3, as shown in Figure 4a. The coordination structure of [Eu(TPPO)$_2$(*D*-facam)$_3$] was categorized to the eight-coordinated square antiprism (SAP).[14a,b,22] The Eu−O bond lengths and bond angles are summarized in Table 4. *D*-facam 3 showed a distorted structure compared with other *D*-facam ligands. As summarized in Table 5, specific selected angles *a* and *b* in *D*-facam 3 (106.2° and 128.7°) were larger than those of *D*-facam 1 (97.9° and 112.0°) and *D*-facam 2 (98.0° and 112.3°). Selected angle *c* in *D*-facam 3 (108.0°) was smaller than that in *D*-facam 1 (118.2°) and *D*-facam 2 (116.6°). The distance between O5 and O6 atoms in *D*-facam 3 (2.91 Å) was relatively larger than those of *D*-facam 1 (2.87 Å) and *D*-facam 2 (2.81 Å) as summarized in Table 4. We also

(20) Hasegawa, Y.; Ohkubo, T.; Sogabe, K.; Kawamura, Y.; Wada, Y.; Nakashima, N.; Yanagida, S. *Angew. Chem., Int. Ed.* **2000**, *39*, 357–360.

(21) (a) Beeby, A.; Clarkson, I. M.; Dickind, R. S.; Faulkner, S.; Parker, D.; Royle, L.; de Sousa, A. S.; Gareth Williams, J. A.; Woods, M. *J. Chem. Soc., Perkin Trans. 2* **1999**, *3*, 193–503. (b) Werts, M. H. V.; Jukes, R. T. F.; Verhoeven, J. W. *Phys. Chem. Chem. Phys.* **2002**, *4*, 1542–1548.

(22) Pavithran, R.; Kumar, N. S. S.; Biju, S.; Reddy, M. L. P.; Junior, S. A.; Freire, R. O. *Inorg. Chem.* **2006**, *45*, 2184–2192.

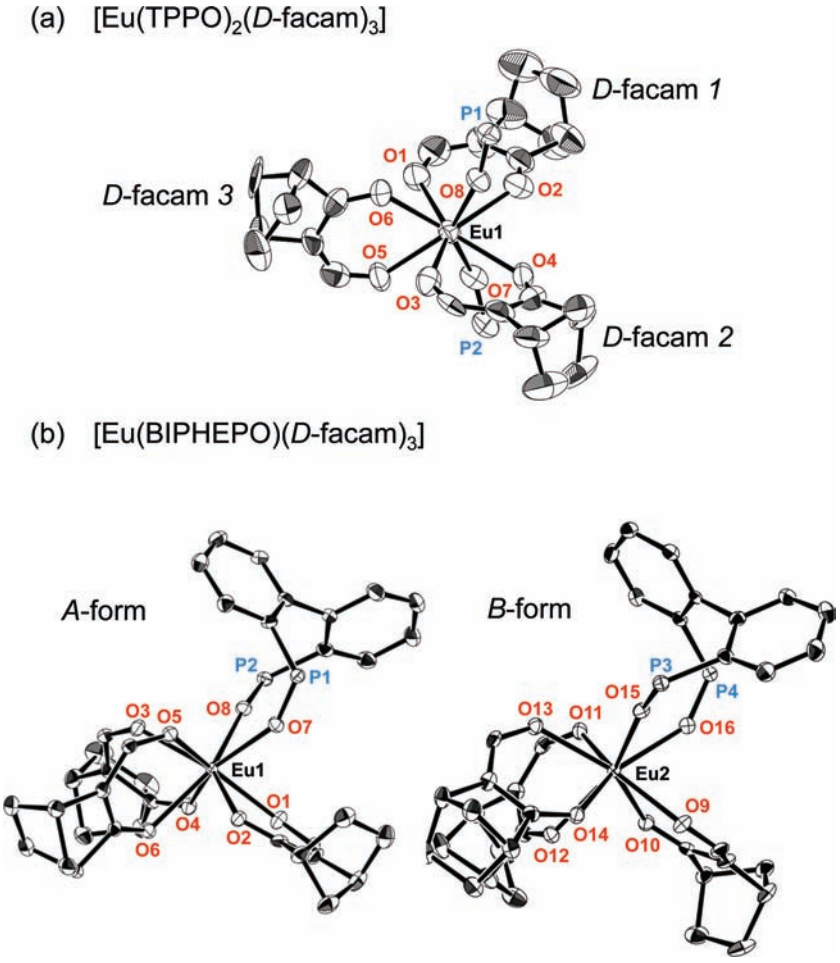

Figure 4. ORTEP views and the coordination structures of (a) [Eu(TPPO)$_2$(*D*-facam)$_3$] and (b) [Eu(BIPHEPO)(*D*-facam)$_3$].

Table 3. Crystal Data, Data Collection, and Structure Refinement for Complexes [Eu(TPPO)$_2$(*D*-facam)$_3$] and [Eu(BIPHEPO)(*D*-facam)$_3$]

	[Eu(TPPO)$_2$-(*D*-facam)$_3$]	[Eu(BIPHEPO)-(*D*-facam)$_3$]
chemical formula	$C_{72}H_{74}EuF_9O_9P_2$	$C_{72}H_{72}EuF_9O_9P_2$
fw	1468.26	1466.25
cryst syst	orthorhombic	monoclinic
space group	P $_{212121}$(#19)	P $_{1211}$ (#4)
a/Å	13.8(7)	13.0(7)
b/Å	18.0(0)	26.5(9)
c/Å	27.8(1)	20.2(4)
α/deg	90.0(0)	90.0(0)
β/deg	90.0(0)	97.4(4)
γ/deg	90.0(0)	90.0(0)
V/Å^3	6946.6(5)	6979.2(2)
Z	4	4
T/K	193.1	103.1
m(Mo Kα)/ cm^{-1}	14.07	14.07
no. of measured reflns	12707	102127
no. of unique reflns	6366	28261
R_{int}	0.0012	0.0037
$R(R_w)$	0.0455 (0.0496)	0.0237 (0.0577)

observed that the distances between the oxygen and the hydrogen atoms in *D*-facam 3 and TPPO ligands, O5−H48 = 2.34 Å and O6−H67 = 2.45 Å, were shorter than sum of van der Waals's radii (< 2.72 Å; Figure 5), suggesting a contribution of hydrogen bonds of P1 and P2 with *D*-facam 3.[23] The distorted geometrical structure of [Eu(TPPO)$_2$(*D*-facam)$_3$] might be caused by the presence of the hydrogen bonding in Eu(III) complexes.

On the other hand, two independent structures were observed in the crystal of [Eu(BIPHEPO)(*D*-facam)$_3$], as illustrated in Figure 4. The geometrical structures of *A* and *B* forms, having (*S*)- and (*R*)- forms of BIPHEPO ligands, respectively, are schematically illustrated in Figure 6. Because of existence of the *D*-facam ligands, these two conformations are not the enantiomers but the diasteromers of each other and should have different photochemical properties. The observed two components' nature in the emission decays of [Eu(BIPHEPO)(*D*-facam)$_3$] might be due to the existence of *A* and *B* forms in acetone-d_6. It should be noted that achiral complexes such as [Eu(BIPHEPO)(hfa)$_3$] show single component decay, which could be attributed to the existence of single emission species or to two enantiomeric isomers having the same emission dynamics. Similar dual exponential decay was also observed for [Eu((*R*/*S*)-BINAPO)(*D*-facam)$_3$], although their X-ray crystallographic analyses could not be achieved. We are expecting a contribution of similar diasteromeric isomers to the emission properties of these complexes. Hydrogen bonds between *D*-facam and BIPHEPO were also observed in [Eu(BIPHEPO)(*D*-facam)$_3$] (see the Supporting Information, CIF file of [Eu(BIPHEPO)(*D*-facam)$_3$]). The combination between *D*-facam and phosphine oxide

(23) Desiraju, G. R.; Steiner, T. *The Weak Hydrogen Bond in Structural Chemistry and Biology*; Oxford University Press: Oxford, U. K., 1999.

Table 4. Selected Distances, Angles, and *S* (Shape Measure Criteria) Angles from the Crystal Structures of $[Eu(TPPO)_2(D\text{-facam})_3]$, *A* Form and *B* Form in $[Eu(BIPHEPO)(D\text{-facam})_3]$

complex	O···O distance/Å	Eu−O distances/Å	O−Eu−O angles/deg	*S* value for SAP: $S(D_{4d})$/deg
$[Eu(TPPO)_2(D\text{-facam})_3]$	O1···O2: 2.87 (*D*-facam *1*)	Eu1−O1: 2.35 Eu1−O2: 2.45	O1−Eu1−O2: 73.3	6.36
	O3···O4: 2.81 (*D*-facam *2*)	Eu1−O3: 2.31 Eu1−O4: 2.46	O3−Eu1−O4: 72.1	
	O5···O6: 2.91 (*D*-facam *3*)	Eu1−O5: 2.39 Eu1−O6: 2.40	O5−Eu1−O6: 74.7	
$[Eu(BIPHEPO)(D\text{-facam})_3]$ *A*-form	O1···O2: 2.90 O3···O4: 2.98 O5···O6: 2.90	Eu1−O1: 2.37 Eu1−O2: 2.46 Eu1−O3: 2.38 Eu1−O4: 2.42 Eu1−O5: 2.36 Eu1−O6: 2.43	O1−Eu1−O2: 73.8 O3−Eu1−O4: 76.9 O5−Eu1−O6: 74.5	7.10
$[Eu(BIPHEPO)(D\text{-facam})_3]$ *B*-form	O9···O10: 2.90 O11···O12: 2.99 O12···O14: 2.89	Eu2−O9: 2.37 Eu2−O10: 2.47 Eu2−O11: 2.37 Eu2−O12: 2.42 Eu2−O13: 2.37 Eu2−O14: 2.44	O9−Eu2−O10: 73.6 O11−Eu2−O12: 77.2 O13−Eu2−O14: 73.7	6.14

Table 5. Selected Angles *a*, *b*, and *c* of *D*-facam Ligands 1, 2, and 3 of $[Eu(TPPO)_2(D\text{-facam})_3]$

ligand	angle *a*/deg	angle *b*/deg	angle *c*/deg
D-facam 1	97.9	112.0	118.2
D-facam 2	98.0	112.3	116.6
D-facam 3	106.2	128.7	108.0

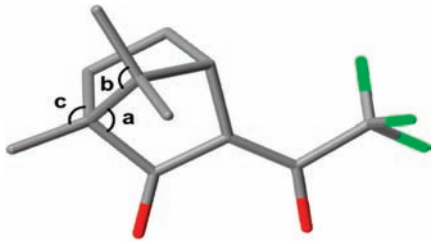

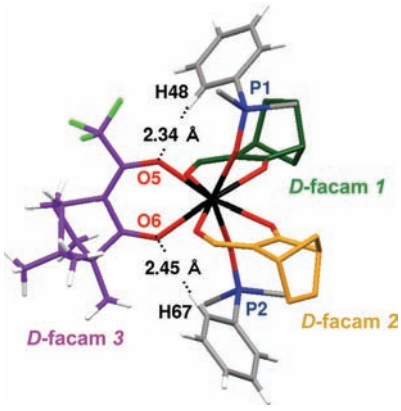

Figure 5. Intramolecular interactions around *D*-facam 1, 2, and 3 in $[Eu(TPPO)_2(D\text{-facam})_3]$. Benzene units containing H48 and H67 atoms in TPPO ligands are shown to illustrate hydrogen bondings of O5−H48 and O6−H67.

ligands seems to provide distorted SAP structures with hydrogen-bond interactions.

In order to estimate the degree of the distorted coordination structures of Eu(III) complexes, we carried out calculations based on the "shape-measure" criterion, the *S* angle.[24] The *S* value is given by

$$S = \min \sqrt{\left[\left(\frac{1}{m}\right)\sum_{i=1}^{m}(\delta_i - \theta_i)^2\right]} \qquad (4)$$

where m, δ_i, and θ_i are the number of possible edges ($m = 18$ for SAP structure), the observed dihedral angle between planes along the *i*th edge, and the dihedral angle for the ideal SAP structure, respectively. The estimated *S* values of $[Eu(TPPO)_2(D\text{-facam})_3]$ and $[Eu(BIPHEPO)(D\text{-facam})_3]$ (*A* and *B* form) are summarized in Table 4 (see Supporting Information, Figure S4, Tables S1 and S2). The *S* value of the *A* form in $[Eu(BIPHEPO)(D\text{-facam})_3]$ (7.10°) was larger than that of $[Eu(TPPO)_2(D\text{-facam})_3]$ (6.36°); the *S* value of the *B* form in $[Eu(BIPHEPO)(D\text{-facam})_3]$ (6.14°) was smaller than that of $[Eu(TPPO)_2(D\text{-facam})_3]$. These estimations indicate that the *A* form in $[Eu(BIPHEPO)(D\text{-facam})_3]$ shows a highly distorted SAP structure compared with $[Eu(TPPO)_2(D\text{-facam})_3]$ and the *B* form in $[Eu(BIPHEPO)(D\text{-facam})_3]$. The highest A_{rel} value of $[Eu(BIPHEPO)(D\text{-facam})_3]$ in our experiments might be caused by the presence of the distorted *A* form with a larger *S* value. The CPL spectrum of $[Eu(BIPHEPO)(D\text{-facam})_3]$ is

(24) Xu, J.; Radkov, E.; Ziegler, M.; Raymond, K. N. *Inorg. Chem.* **2000**, *39*, 4156–4164.

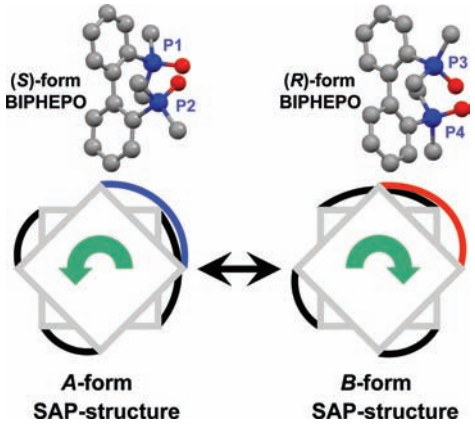

Figure 6. Two coordination structures (*A* and *B* forms) of [Eu(BIPHEPO)(*D*-facam)$_3$] and the corresponding structures of BIPHEPO ligands.

observed as a sum spectrum of CPL signals from the *A* form (left-twisted SAP) and *B* form (right-twisted SAP). The dissymmetry factor of [Eu(BIPHEPO)(*D*-facam)$_3$] would be affected by quasi-racemization with the diastereomeric isomers of the *A* form ($S = 7.10°$) and *B* form ($S = 6.14°$). We conclude that the largest dissymmetry factor of the CPL spectrum in enantiopure [Eu(TPPO)$_2$(*D*-facam)$_3$] should be induced by their characteristic distorted structure ($S = 6.36°$), which is related to an increase of the electric-dipole transition probability.

Conclusion

The large g_{CPL} value at the magnetic-dipole transition of the chiral Eu(III) complex is contributed to the perturbation from the enhanced electric-dipole transition and is directly linked to the distorted asymmetric coordination structures around the Eu(III) ions. In this study, we used acetone-d_6 as a solvent for the enhancement of emission properties. The emission spectral shapes related to the electric-dipole transition also depend on the solvent species. The emission spectral shapes are directly linked to CPL properties. Thus, CPL properties might be influenced by the characteristics of the solvent.

In this study, we observed the diasteromeric SAP structures of the chiral Eu(III) complex with bidentate phosphine oxide. The enantiopure Eu(III) complex composed of (*R*/*S*)-BINAPO and *D*-facam shows promise toward the enhancement of the g_{CPL} value in CPL properties. A study on enantiopure luminescent lanthanide complexes with a distorted asymmetric structure is expected to contribute a better understanding of CPL properties.

Acknowledgment. This work was supported partly by a Giant-in-Aid for Scientific Research on Priority Area of "Strong Photon-Molecule Coupling Fields for Chemical Reactions" and "Emergent chemistry of nano-scale molecular systems" from Ministry of Education, Culture, Sports, Science and Technology (MEXT), Japan.

Supporting Information Available: Additional CD spectra of (*R*/*S*)-BINAPO, the calculations of the CD spectra, the normalized emission and the CPL spectra of [Eu((*S*)-BINAPO)(*D*-facam)$_3$] and [Eu(BIPHEPO)(*D*-facam)$_3$], calculation of *S* values for [Eu(TPPO)$_2$(D-facam)$_3$] and two forms of [Eu(BIPHEPO)(D-facam)$_3$]; Figures S1−S4 and Table S1−S2. X-ray crystallographic data (CIF files) of [Eu(TPPO)$_2$(*D*-facam)$_3$] and [Eu(BIPHEPO)(*D*-facam)$_3$]. This material is available free of change via Internet at http://pubs.acs.org.